Available online at www.sciencedirect.com
SCIENCE DIRECT
Polymer 46 (2005) 4355–4360
polymer
www.elsevier.com/locate/polymer

Molecular modelling of the stress–strain behaviour of elastomers in pure shear

J.I. Cail, R.F.T. Stepto*

Polymer Science and Technology Group, School of Materials, The University of Manchester, Grosvenor Street, Manchester, M1 7HS, UK

Available online 7 April 2005

Dedicated, with best wishes, to Professor James E. Mark on the occasion of his 70th birthday

Abstract

It is demonstrated that experimental stress–strain data for several types of polymer network under pure shear display an approximately universal behaviour. The Monte–Carlo network-modelling method of Stepto, Taylor and Cail is extended to treat stress–strain behaviour in pure shear and its predictions are in good agreement with the experimental data. The predictions of Gaussian network theory are shown to be seriously in error.

Keywords: Polymer networks; Pure shear; Monte–Carlo modelling

1. Introduction

The stress–strain behaviour of elastomers is commonly investigated in uniaxial extension or compression. Generally, the experimental stress–strain curves show reductions in modulus as strain increases and it is possible to reproduce them using a variety of theoretical and modelling approaches [1,2]. However, the situation regarding the interpretation of biaxial stress–strain behaviour is not so satisfactory, with several authors finding that a variety of theoretical approaches were unable to predict experimental stress–strain data for various elastomers [3–6].

A form of biaxial deformation frequently studied is pure shear, achieved by uniaxial extension with the material sample held at constant width. If λ_1 is the deformation ratio in the (principal) strain direction and λ_2 and λ_3 are the deformation ratios perpendicular to the strain direction then, for an incompressible material in pure shear,

$$\lambda_2 = 1 \text{ and } \lambda_3 = 1/\lambda_1. \quad (1)$$

Pure shear is distinct from simple shear, for which Eqs. (1) also hold, in that the principal axes (1,2,3) do not rotate on deformation.

The present paper demonstrates for the first time that published experimental stress–strain data determined under pure shear for natural rubber (NR) [7], poly(vinyl chloride) (PVC) [5] and poly(ethylene terephthalate) (PET) [6] display an approximately universal behaviour. This universal behaviour is compared with the classical predictions of Gaussian elasticity theory [1,8] and with the predictions of an extension of the Monte–Carlo (MC) network-modelling method of Stepto, Taylor and Cail [9–11]. The MC approach can be regarded as ab initio network modelling. The only parameters it uses are those of the rotational-isomeric-state (RIS) model for the individual network chains. The approach has been used previously to give quantitative predictions of the uniaxial stress–strain behaviour of poly(dimethyl siloxane) [9], polyethene (PE) [10,11] and PET [12], and the stress-optical behaviour of PE [11,13]. This paper does not discuss the use of generalised strain–energy functions [1,3,8] as it is concerned with molecular rather than phenomenological interpretations of the experimental data.

2. Biaxial deformation of a Gaussian network

This section summarises standard relationships [1,8] related to the biaxial deformation of a Gaussian network. The change of Helmholtz energy, ΔA, on deformation at

* Corresponding author.

0032-3861/$ - see front matter © 2005 Elsevier Ltd. All rights reserved.
doi:10.1016/j.polymer.2005.02.038

constant volume is

$$\Delta A = (1/2)X(\lambda_1^2 + \lambda_2^2 + \lambda_3^2 - 3), \tag{2}$$

where $X = NkT$; with N the number of elastic chains in the network. The condition of constant volume, $\lambda_1\lambda_2\lambda_3 = 1$, also gives for deformation along the unconstrained axis, 3,

$$\lambda_3 = \frac{1}{\lambda_1\lambda_2}. \tag{3}$$

hence,

$$\Delta A = (1/2)X\left(\lambda_1^2 + \lambda_2^2 + \frac{1}{\lambda_1^2\lambda_2^2} - 3\right). \tag{4}$$

Differentiation of Eq. (4) with respect to l_1 and l_2, the deformed lengths of the network along axes 1 and 2, gives the elastic force, f_1, along axis 1 (λ_2 constant)

$$f_1 = \frac{\partial \Delta A}{\partial l_1} = \left(\frac{\partial \Delta A}{\partial \lambda_1}\right)\frac{1}{l_1^o} = \frac{X}{2l_1^o}\left(2\lambda_1 - \frac{2}{\lambda_2^2}\times\frac{1}{\lambda_1^3}\right) \tag{5}$$

and the elastic force along axis 2 (λ_1 constant)

$$f_2 = \frac{\partial \Delta A}{\partial l_2} = \left(\frac{\partial \Delta A}{\partial \lambda_2}\right)\frac{1}{l_2^o} = \frac{X}{2l_2^o}\left(2\lambda_2 - \frac{2}{\lambda_1^2}\times\frac{1}{\lambda_2^3}\right). \tag{6}$$

l_1^o and l_2^o are the undeformed lengths of the network.

The nominal stress along axis 1, σ_1, is

$$\sigma_1 = \frac{X}{V_o}\left(\lambda_1 - \frac{1}{\lambda_2^2}\times\frac{1}{\lambda_1^3}\right) = G\left(\lambda_1 - \frac{1}{\lambda_2^2}\times\frac{1}{\lambda_1^3}\right) \tag{7}$$

and the nominal stress along axis 2, σ_2, is

$$\sigma_2 = \frac{X}{V_o}\left(\lambda_2 - \frac{1}{\lambda_1^2}\times\frac{1}{\lambda_2^3}\right) = G\left(\lambda_2 - \frac{1}{\lambda_1^2}\times\frac{1}{\lambda_2^3}\right), \tag{8}$$

where V_o is the sample volume and G is the shear modulus, with

$$G = \frac{X}{V_o} = \frac{NkT}{V_o}. \tag{9}$$

The ratio of nominal stresses is

$$\frac{\sigma_1}{\sigma_2} = \frac{\lambda_2(\lambda_1^4\lambda_2^2 - 1)}{\lambda_1(\lambda_1^2\lambda_2^4 - 1)}. \tag{10}$$

The true stresses, t_1 and t_2, are simply related to the nominal stresses through the relationships $t_1 = \sigma_1\lambda_1$ and $t_2 = \sigma_2\lambda_2$, giving, from Eqs. (7), (8) and (10),

$$t_1 = G\left(\lambda_1^2 - \frac{1}{\lambda_2^2}\times\frac{1}{\lambda_1^2}\right),\ t_2 = G\left(\lambda_2^2 - \frac{1}{\lambda_1^2}\times\frac{1}{\lambda_2^2}\right) \tag{11}$$

and

$$\frac{t_1}{t_2} = \frac{(\lambda_1^4\lambda_2^2 - 1)}{(\lambda_1^2\lambda_2^4 - 1)}. \tag{12}$$

In addition,

$$t_1 - t_2 = G(\lambda_1^2 - \lambda_2^2). \tag{13}$$

The equations discussed so far describe general biaxial deformation, subject only to the conditions of constant volume and no stress applied along axis 3. For pure shear, Eqs. (1) hold and from Eqs. (4), (7), (8), (10), (11–13)

$$\Delta A = (1/2)X\left(\lambda_1^2 + \frac{1}{\lambda_1^2} - 2\right) \tag{14}$$

$$\sigma_1 = G\left(\lambda_1 - \frac{1}{\lambda_1^3}\right),\ \sigma_2 = G\left(1 - \frac{1}{\lambda_1^2}\right) \tag{15}$$

$$\frac{\sigma_1}{\sigma_2} = \frac{(\lambda_1^4 - 1)}{\lambda_1(\lambda_1^2 - 1)} \tag{16}$$

$$t_1 = G\left(\lambda_1^2 - \frac{1}{\lambda_1^2}\right),\ t_2 = G\left(1 - \frac{1}{\lambda_1^2}\right)(= \sigma_2) \tag{17}$$

$$\frac{t_1}{t_2} = \frac{(\lambda_1^4 - 1)}{(\lambda_1^2 - 1)} \tag{18}$$

$$t_1 - t_2 = G(\lambda_1^2 - 1) \tag{19}$$

Eqs. (13) and (19), or their extensions based on generalised strain–energy functions, have been used [3,8] as bases for discussions and interpretations of biaxial and pure-shear stress–strain behaviour. However, they have the disadvantage that a value for G (assuming Gaussian behaviour is followed) or its generalisation is needed. In contrast, Eqs. (10), (12), (16) and (18) (or their generalisations) can be used to discuss biaxial and pure-shear behaviour, to a first approximation independent of the value of G or its variation with deformation. Eq. (18) has the further advantage that de l'Hôpital's rule gives

$$\lim_{\lambda_1 \to 1}(t_1/t_2) = \lim_{\lambda_1 \to 1}(4\lambda_1^3/2\lambda_1) = 2. \tag{20}$$

This limiting value of the ratio t_1/t_2 will hold for undeformed (bulk) networks that obey the assumptions of a Gaussian network, namely, random chain orientation and a probability density distribution function of network chain end-to end distances (r) of Gaussian form ($\propto e^{-r^2}$) for values of r not near full extension. Hence, the limiting value of 2 can be expected to be of wide validity.

3. Monte–Carlo (MC) network modelling for pure shear

The algorithm for the MC network modelling has been described previously in relation to uniaxial stress–strain and stress–optical behaviour [9–12]. Only a summary will be given here, together with a description of the developments needed to model network stress–strain behaviour under pure shear.

3.1. Calculation and representation of elastic Helmholtz energy change

In the first stage of the Monte–Carlo (MC) simulation, an RIS chain model is used to generate the radial end-to-end distance distribution, $W(r)$, for the network chains of a given number of skeletal bonds (n) at a given temperature. $W(r)$ is constructed as a histogram and the corresponding values of probability density, $P(\mathbf{r})$, are evaluated as $W(r)/4\pi r^2$, assuming the random orientation of chains in three dimensions.

The second stage of the simulation concerns the elastic behaviour of the network, represented by a sample of independent, initially randomly oriented individual chains in a Cartesian laboratory-reference frame (axes 1, 2 and 3) with one end of each chain fixed at the origin.

A chain, i, with end-to-end distance $r_{o,i}$, is first chosen in proportion to $W(r_{o,i})$. The 1- and 2- co-ordinates of its 'free' chain end are chosen randomly, and the 3-component defined consistent with $\mathbf{r}_{o,i}$. That is,

$$\boldsymbol{r}_{o,i} = (r_{o1,i}, r_{o2,i}, r_{o3,i}) \tag{21}$$

with

$$r_{o,i}^2 = r_{o1,i}^2 + r_{o2,i}^2 + r_{o3,i}^2. \tag{22}$$

Deformations, using a series of values of λ_1 along axis 1, subject to $\lambda_2 = 1$ and $\lambda_3 = 1/\lambda_1$, are made and the deformed end-to-end distances, r_{def}, calculated by simple geometry. The end-to-end distance is allowed to increase only up to its effective, conformational maximum, r^*_{max}, above which $W(r) = 0$ according to the sampled $W(r)$. Any values of r_{def} in excess of r^*_{max} are put equal to r^*_{max}, thus limiting r to the range of values determined by the bond-conformational energies, consistent with $W(r)$ and automatically introducing the overall non-affine behaviour of chains in the network. The value of $W(r_{def})$ associated with r_{def} is ascertained from $W(r)$, and $\ln P(r_{def})$ evaluated.

The Helmholtz energy change upon deformation is assumed to arise solely from the corresponding entropic change. Hence, for chain i,

$$\Delta A_{chain,i}/kT = \ln\{P(\boldsymbol{r}_{o,i})/P(\boldsymbol{r}_{def,i})\}, \tag{23}$$

The average change per chain at each λ_1 is calculated as

$$\Delta A/NkT = \frac{1}{N}\sum_{i=1}^{N} \Delta A_{chain,i} = \frac{1}{N}\sum_{i=1}^{N} \ln\{P(\boldsymbol{r}_{o,i})/P(\boldsymbol{r}_{def,i})\}, \tag{24}$$

where N is the number of chains in the MC sample (i.e. network). Typically $N = 3$ to 5×10^6.

Generalising Eq. (14), the Helmholtz energy change accompanying a macroscopic deformation of λ_1 can be expressed as

$$\Delta A/NkT = s\left(\lambda_1^2 + \frac{1}{\lambda_1^2} - 2\right). \tag{25}$$

For Gaussian (affine) networks [1,8], $s = 1/2$, and a plot of $\Delta A/NkT$ versus $\lambda_1^2 + 1/\lambda_1^2 - 2$ for pure shear is linear with a slope of 1/2. The non-affine chain behaviour that arises automatically under the chain-deformation scheme means that s is a function of λ_1. The function is conveniently expressed as a polynomial in λ_1 so that it can be differentiated analytically to determine the elastic force. Eq. (25) is analogous to that used previously [9–12] for a uniaxial deformation λ, except that the function multiplying s was then $\lambda^2 + 2/\lambda - 3$.

The non-affine network chain behaviour that occurs can be viewed as a kind of orientation effect. Chains in the relaxed network, whose end-to-end vectors lie close to the extension axis become conformationally fully extended at low macroscopic strains, and hence contribute nothing more to the Helmholtz energy change of the network as deformation increases further; more of the strain is effectively 'taken-up' by network chains whose end-to-end vectors lie at ever-increasing angles from the extension axis. The phenomenon manifests itself as a reduction in the rate of Helmholtz energy change per chain with increasing macroscopic deformation.

3.2. Calculation of stress along axis 1

Eq. (25) can be expressed in terms of molar quantities, with

$$\frac{\Delta A}{RT\rho}\frac{1}{V_o} = \frac{s}{M_c}\left(\lambda_1^2 + \frac{1}{\lambda_1^2} - 2\right), \tag{26}$$

where ρ is the density of the network and M_c is the network-chain molar mass. Differentiation of Eq. (26) with respect to network length, l_1, yields the reduced elastic force, $f_1/RT\rho$, with

$$\frac{f_1}{RT\rho}\frac{1}{V_o} = \frac{1}{l_1^o M_c}\left(2s(\lambda_1 - 1/\lambda_1^3) + (\lambda_1^2 + 1/\lambda_1^2 - 2)\frac{ds}{d\lambda_1}\right). \tag{27}$$

The reduced nominal stress, $\sigma_1/RT\rho$, can then be found by using the relationship $a_{23}^o l_1^o = V_o$, where a_{23}^o is the initial cross-sectional area perpendicular to axis 1. Thus,

$$\frac{\sigma_1}{RT\rho} = \frac{f_1}{RT\rho a_{23}^o} = \frac{1}{M_c}\left(2s(\lambda_1 - 1/\lambda_1^3) + (\lambda_1^2 + 1/\lambda_1^2 - 2)\frac{ds}{d\lambda_1}\right) \tag{28}$$

and the true stress

$$t_1 = \sigma_1\lambda_1$$

$$= \frac{1}{M_c}\left(2s(\lambda_1^2 - 1/\lambda_1^2) + (\lambda_1^3 + 1/\lambda_1 - 2\lambda_1)\frac{ds}{d\lambda_1}\right). \quad (29)$$

3.3. Calculation of stress along axis 2

Because there is zero deformation of the network along axis 2, incremental probe deformations of the individual chains are used to determine directly the rate of change of Helmholtz energy with deformation and, hence, the elastic force needed to maintain $\lambda_2 = 1$. After deformation along axis 1, chain i, with undeformed end-to-end vector $\boldsymbol{r}_{o,i}$ (Eqs. (21) and (22)), has been deformed to

$$\boldsymbol{r}_{def,i} = (r_{def1,i}, r_{def2,i}, r_{def3,i}) = (r_{o1,i}\lambda_1, r_{o2,i}, r_{o3,i}/\lambda_1). \quad (30)$$

With λ_1 kept constant, incremental deformation ratios $\delta\lambda_2^+$ and $\delta\lambda_2^-$ are applied along the 2 axis, with $\delta\lambda_2^+$ (>1) increasing $r_{o2,i}$ and $\delta\lambda_2^-$ (<1) decreasing $r_{o2,i}$, to give

$$\boldsymbol{r}^+_{def,i} = (r_{def1,i}, r_{def2,i}\delta\lambda_2^+, r_{def3,i}/\delta\lambda_2^+) \quad (31)$$

and

$$\boldsymbol{r}^-_{def,i} = (r_{def1,i}, r_{def2,i}\delta\lambda_2^-, r_{def3,i}/\delta\lambda_2^-). \quad (32)$$

The incremental changes in $r_{def2,i}$ are

$$\delta r^+_{def2,i} = (\delta\lambda_2^+ - 1)r_{def2,i}$$

and

$$\delta r^-_{def2,i}, = (\delta\lambda_2^- - 1)r_{def2,i}. \quad (33)$$

The changes in Helmholtz energy are then evaluated through the probability density functions with

$$\delta_2^+ \ln P(\boldsymbol{r}_{def,i}) = \ln P(\boldsymbol{r}^+_{def,i}) - \ln P(\boldsymbol{r}_{def,i}) \quad (34)$$

and

$$\delta_2^- \ln P(\boldsymbol{r}_{def,i}) = \ln P(\boldsymbol{r}^-_{def,i}) - \ln P(\boldsymbol{r}_{def,i}). \quad (35)$$

The elastic force exerted by chain i is evaluated using finite differences, giving

$$\frac{f^+_{2,i}}{kT} = \frac{-\delta_2^+ \ln P(\boldsymbol{r}_{def,i})}{\delta r^+_{def2,i}} \text{ and } \frac{f^-_{2,i}}{kT} = \frac{-\delta_2^- \ln P(\boldsymbol{r}_{def,i})}{\delta r^-_{def2,i}}, \quad (36)$$

with the average of $f^+_{2,i}$ and $f^-_{2,i}$ being taken as the value of the force

$$f_{2,i} = 1/2(f^+_{2,i} + f^-_{2,i}). \quad (37)$$

The average force per chain is then given by the sum over the MC sample with

$$f_{2,chain} = \frac{1}{N}\sum_{i=1}^{N} f_{2,i} \quad (38)$$

The number of chains per unit volume in the network equals $\rho N_{Av}/M_c$ and the number of chains per unit undeformed area normal to a principal axis equals $(\rho N_{Av}/M_c)^{2/3}$. Hence, the nominal stress along axis 2, σ_2, is given directly by the equation

$$\sigma_2 = f_{2,chain}(\rho N_{Av}/M_c)^{2/3}. \quad (39)$$

In addition, $\sigma_2 = t_2$ as $\lambda_2 = 1$.

4. Results and discussion

Fig. 1 presents the ratio of true stresses in pure shear, t_1/t_2, plotted versus deformation ratio λ_1. The experimental values are derived from published data [5–7] on various polymers. The prediction of Gaussian network theory, Eq. (18), is also shown and the results from the present MC network modelling according to Eqs. (29) and (39). To within experimental error, the experimental results define an essentially linear universal relationship and the plot given by the present MC network modelling is in agreement with the relationship. For the network modelling, values of $\delta\lambda_2^+$ and $\delta\lambda_2^-$ of 1.04 and 0.96, respectively, were used to give negligible numerical scatter, and PE chains of 100 bonds at 403 K were chosen because their probability density function, $P(r)$, and radial distribution function, $W(r)$, were already available from previous work [10,11]. The universal behaviour shown in Fig. 1 indicates that the choice of type of chain was not critical. However, the sensitivity to chain structure of the relationship between t_1/t_2 and λ_1 will be the subject of future investigations.

It is clear that Gaussian theory is seriously in error. The essentially quadratic relationship of Eq. (18) gives too strong a dependence of t_1/t_2 on λ_1. However, as expected (see discussion of Eq. (20)), the limiting value of 2 at λ_1 is seen to be consistent with experiment and the MC simulations. The reason why Gaussian network theory overestimates the value of t_1/t_2 at a given λ_1 can be seen from a comparison of the elastic Helmholtz energies for Gaussian and real chains in dependence on chain extension. Such a comparison is shown in Fig. 2 for PE chains.

The curves for the real chains have larger negative slopes than the linear Gaussian plots. Such relative behaviour is true for most types of flexible polymer chains. When evaluating t_2 using the MC modelling and the incremental deformations $\delta\lambda_2^+$ and $\delta\lambda_2^-$, the larger slopes result in larger changes in Helmhotz energy and, hence, larger values of t_2 and smaller values of t_1/t_2 than those predicted assuming Gaussian behaviour. The continuing increase in negative slope with chain extension apparent in Fig. 2 also means that the deviation of the Gaussian values of t_1/t_2 from the actual values increases as the networks are deformed. It should be noted that in the deformation of chains in the determination of t_1 some chains reach full extension and, hence, reduce stress as λ_1 increases. In contrast, because chains do not reach full extension in the determination of t_2, the curvature of the Helmholtz energy plot, as shown in Fig. 2, is the dominant factor.

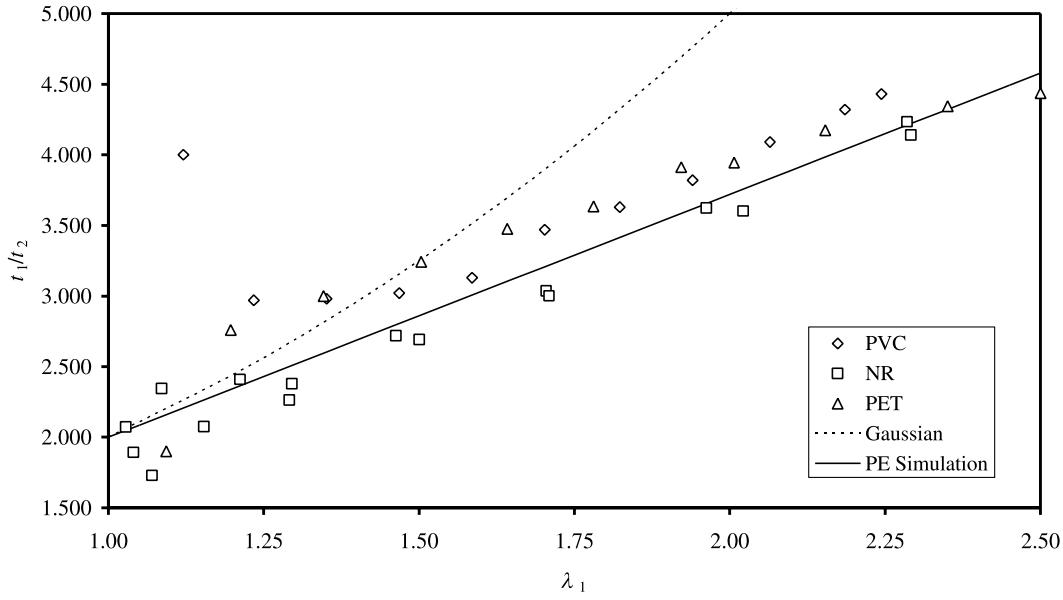

Fig. 1. Ratio of true stresses in pure shear, t_1/t_2, versus λ_1, the deformation ratio along principal axis 1. Experimental data: PVC [5], NR [7] and PET [6], prediction according to Gaussian network theory, Eq. (18). Prediction according to MC network modelling, Eqs. (29) and (39), for a PE network of 100-bond chains at 403 K using the Abe–Jernigan–Flory RIS model [14].

5. Conclusions

The ratio of experimentally determined principal stresses of polymer networks in pure shear, t_1/t_2, is shown to be approximately universally related to network extension, λ_1. MC network modelling gives results that are in agreement with experiment. In contrast, and for reasons that can be understood, Gaussian network theory greatly overestimates the values of t_1/t_2. However, as expected, the limiting value of $t_1/t_2=2$ at $\lambda_1=1$ from Gaussian theory is in agreement with the results of experiment and the MC modelling.

Acknowledgements

The support of the EPSRC is gratefully acknowledged and also access to the Accelrys Polymer software for the background RIS calculations.

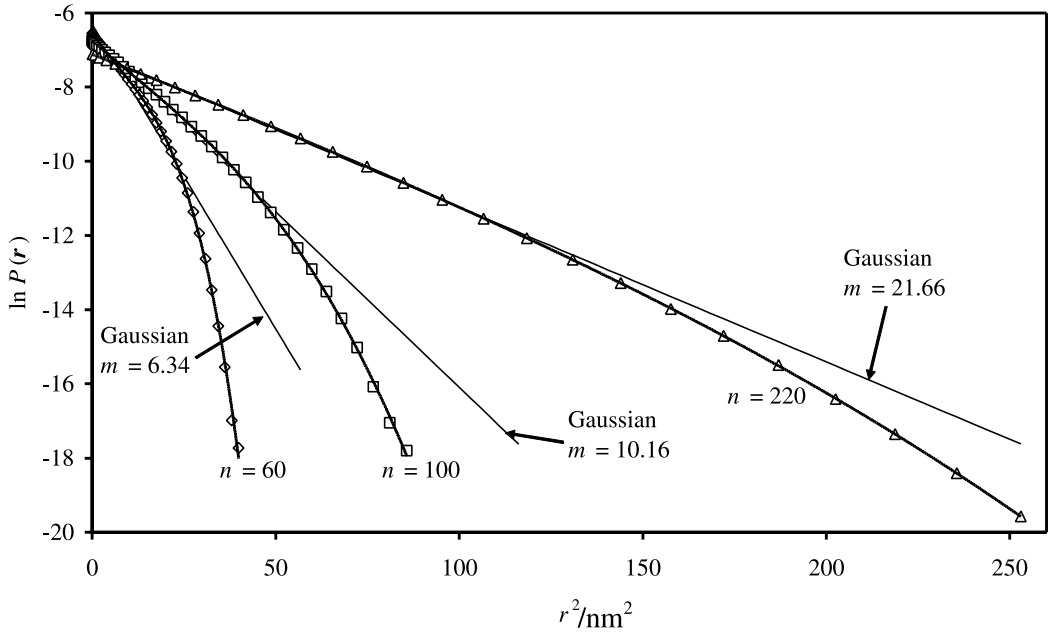

Fig. 2. Elastic Helmholtz energy, $\ln P(\mathbf{r})(=-\Delta A/kT)$, *versus* the square of the end-to-end distance, r^2, for PE chains of various lengths using the same RIS model and temperaure as in Fig. 1. The number of skeletal bonds, n, in each chain is indicated along with the number of freely-jointed links, m, in the equivalent Gaussian chain having the same fully-extended length and mean-square end-to-end distance as the real chain.

References

[1] Mark JE, Erman B. In: Stepto RFT, editor. Polymer networks—principles of their formation structure and properties. London: Blackie Academic and Professional; 1998 [Chapter 7].
[2] Gottlieb M, Gaylord RJ. Polymer 1983;24:1644.
[3] Gottlieb M, Gaylord RJ. Macromolecules 1987;20:130.
[4] Treloar LRG. Br Polym J 1982;14:121.
[5] Sweeney J, Ward IM. Trans IChem E 1993;71:232.
[6] Matthews RG, Duckett RA, Ward IM, Jones DP. Polymer 1997;38:4795.
[7] Jones DF, Treloar LRG. J Phys D: Appl Phys 1975;8:1285.
[8] Treloar LRG. The physics of rubber elasticity. 3rd ed. Oxford: Oxford University Press; 1975.
[9] Stepto RFT, Taylor DJR. Macromol Symp 1995;93:261.
[10] Stepto RFT, Taylor DJR. J Chem Soc, Faraday Trans 1995;91:2369.
[11] Taylor DJR, Stepto RFT, Jones RA, Ward IM. Macromolecules 1999;32:1978.
[12] Cail JI, Stepto RFT. Polymer 2003;44:6077.
[13] Cail JI, Taylor DJR, Stepto RFT, Brereton MG, Jones RA, Ries ME, Ward IM. Macromolecules 2000;33:4966.
[14] Abe A, Jernigan RL, Flory PJ. J Amer Chem Soc 1966;88:631.